



HAL
open science

A new foam-based method for the (bio)degradation of hydrocarbons in contaminated vadose zone

I. Bouzid, D. Pino Herrera, M. Dierick, Y. Pechaud, V. Langlois, P.Y. Klein,
J. Albaric, N. Fatin-Rouge

► **To cite this version:**

I. Bouzid, D. Pino Herrera, M. Dierick, Y. Pechaud, V. Langlois, et al.. A new foam-based method for the (bio)degradation of hydrocarbons in contaminated vadose zone. *Journal of Hazardous Materials*, 2021, 401, pp.123420. 10.1016/j.jhazmat.2020.123420 . hal-02962558

HAL Id: hal-02962558

<https://hal.science/hal-02962558v1>

Submitted on 18 Jul 2022

HAL is a multi-disciplinary open access archive for the deposit and dissemination of scientific research documents, whether they are published or not. The documents may come from teaching and research institutions in France or abroad, or from public or private research centers.

L'archive ouverte pluridisciplinaire **HAL**, est destinée au dépôt et à la diffusion de documents scientifiques de niveau recherche, publiés ou non, émanant des établissements d'enseignement et de recherche français ou étrangers, des laboratoires publics ou privés.



Distributed under a Creative Commons Attribution - NonCommercial 4.0 International License

1 A new foam-based method for the (bio)degradation of hydrocarbons
2 in contaminated vadose zone

3 *I. Bouzid^a, D. Pino Herrera^b, M. Dierick^c, Y. Pechaud^b, V. Langlois^b, P.Y. Klein^c, J. Albaric^d, N. Fatin-*
4 *Rouge^a*

5 ^a Université de Bourgogne Franche-Comté–Besançon, Institut UTINAM–UMR CNRS 6213, 16, route
6 de Gray, 25030, Besançon, France

7 ^b Université Paris-Est, Laboratoire Géomatériaux et Environnement (LGE), EA 4508, UPEM, 77454
8 Marne-la-Vallée, France

9 ^c REMEA, 22 Rue Lavoisier, 92000 Nanterre, France

10 ^d Laboratoire de Chrono-Environnement, UMR CNRS 6249, Université de Bourgogne, Franche-Comté,
11 France

12 Corresponding author: Nicolas Fatin-Rouge

13 E-mail: nicolas.fatin-rouge@univ-fcomte.fr

14 Telephone: +33 3 81 66 20 91

15

16 Abstract

17 An innovative foam-based method for Fenton reagents (FR) and bacteria delivery was
18 assessed for the *in situ* remediation of a petroleum hydrocarbon-contaminated unsaturated
19 zone. The surfactant foam was first injected, then reagent solutions were **delivered** and
20 propagated through the network of foam lamellae with a piston-like effect. Bench-scale

21 experiments demonstrated the feasibility of the various treatments with hydrocarbon (HC)
22 removal efficiencies as high as 96%. Compared to the direct injection of FR solutions, the
23 foam-based method led to larger radii of influence and more isotropic reagents delivery,
24 whereas it did not show any detrimental effect regarding HC oxidation. Despite 25% of HCs
25 were expelled from the treated zone because of high foam viscosity, average degradation
26 rates were increased by 20%. At field-scale, foam and reagent solutions injections in soil
27 were tracked both using visual observation and differential electric resistivity tomography.
28 The latter demonstrated the controlled delivery of the reactive solutions using the foam-
29 based method. Even if the foam-based method duration is about 5-times longer than the
30 direct injection of amendment solutions, it provides important benefits, such as the
31 confinement of harmful **volatile hydrocarbons** during Fenton treatments, the enhanced
32 reagents delivery and the 30% lower consumption of the latter.

33

34 1. Introduction

35 Contamination of soils by petroleum hydrocarbons (HCs) is a worldwide concern, given the
36 health and environmental hazards [1]. Their occurrence in the environment is often linked to
37 anthropogenic activities, such as accidental spills and leaks [2,3]. In France, half of the
38 polluted sites are contaminated by HCs, while polycyclic aromatic hydrocarbons (PAHs) are
39 involved in more than 15% of the cases [4]. *In situ* environmental remediation (ISER) is
40 increasingly used among remediation strategies because of the lower dissemination risks
41 and the higher sustainability. The application of In Situ Chemical Oxidation (ISCO)
42 technologies has shown to be a good strategy for the remediation of these contaminated
43 sites [5]. Among the various ISCO treatment methods, Fenton oxidation is the most
44 commonly used [6]. Fenton oxidation uses the reaction of hydrogen peroxide solution and
45 the ferrous ion to produce the highly reactive hydroxyl radical (eq. 1), for HC mineralization.



47 Recently, it was suggested that since ISCO is often not able to access and oxidize all of the
48 residual contaminants, biological polishing would be a good means to complete at low cost
49 the remediation of contaminated sites [7–11]. Fenton reagent (FR) appears to be an
50 excellent candidate for the oxidation step, because of the environmental friendliness of its
51 decomposition products and its low persistence in the environment [11–15]. Moreover,
52 Fenton oxidation decreases pollutants concentrations and improves the bioavailability of
53 metabolites, which facilitates indigenous bacterial activity [16–19]. Finally, it also provides
54 oxygen and nutrients for indigenous bacteria to improve the biodegradation of pollutants
55 [11,17]. Besides, *in situ* bioremediation treatments alone have a limited effectiveness to
56 remediate historically contaminated soils. Usually, HCs are strongly sorbed onto (or

57 partitioned into) solid phases and are thus not easily degraded by microorganisms. Then, in
58 order to be degraded, HCs must be released into the aqueous phase [20]. Due to the low
59 mass-transfer rates in the soil matrix, this release often limits the effectiveness of
60 bioremediation. *In situ* bioremediation as post-treatment improved HCs removal and
61 reduced the soil toxicity after a chemical treatment, which meets the revitalization goals
62 [21]. Nevertheless, more research is required to further study and optimize the interaction
63 between the two treatments (operating conditions, micro-organisms, etc.). Basic
64 bioremediation methods include biostimulation (BS) and bioaugmentation (BA) [22,23]. They
65 have a minimal environmental impact and low processing costs [24]. However, the
66 degradation efficiency is often hindered by the poor contact between remedial agents and
67 contaminants, especially in the vadose zone where gravity and anisotropy may hinder the
68 distribution of amendments [25–27].

69 Currently, there is a growing interest for the use of high viscosity shear-thinning fluids for
70 ISER. Among them, surfactant foam has shown to be promising [25,26,28–33]. Foam in
71 porous media appears as gas bubbles separated by thin liquid films (lamellae) blocked at
72 pore throats. These lamellae must stretch to go through pores or break, opposing resistance
73 to gas flow. This gives an important apparent viscosity to strong foams that diverts flow from
74 big pores to smaller ones [34]. Hence, foam can be used in two ways, as a blocking agent
75 [31,35], or, as a mobility control agent to avoid the digitation of the injected fluid or related
76 phenomena [25,26,33,36]. So far, reports about field-scale remediation tests dealing with
77 foams are scarce and only mention aquifers contaminated by chlorinated-compounds
78 [29,31,37]. The occurrence of HC contaminations and challenging specific issues, like radius
79 of influence (ROI which is the radial distance travelled by the fluid from the injection point)
80 in vadose zones, and the efficiency of degradation reactions, deserve studies.

81 Previously, we reported some bench-scale developments of this innovative surfactant foam-
82 based technology, considering the improved oxidation of coal-tar contaminated soils by
83 persulfate [25,26,28,38]. In this case, further critical developments are reported, considering
84 historically HC contaminated soils, the control and performance of the powerful Fenton
85 reaction and of its combined treatment with biodegradation, assessed *in situ* both at bench
86 and field-scales. First, a comparative study in sandboxes of amendment delivery and HC
87 degradation rates using Fenton in acidic conditions is provided, considering the new foam-
88 based technology vs. the usual direct injection of active solutions. Second, combined Fenton
89 in non-acidified conditions and biological treatments applied as a post-oxidation treatment
90 are reported. Finally, the application of the combined treatment at the real scale using this
91 new technology is reported and assessed, also considering a cost-benefit-risk balance. Even
92 if they are scarce, all the reported assessments of foam-based treatments in ISER have
93 highlighted the technical difficulties to properly manage this complex fluid [29,31,35]. For
94 this reason, a geophysical imaging using the low-invasive electrical resistivity tomography
95 (ERT) was carried out to monitor the propagation of the injected fluids, during our field tests.

96

97 2. Materials and methods

98 2.1. Test-site and soils

99 The **study** site was a former petroleum hydrocarbon storage area, **situated** in Collonges-au-
100 Mont-d'Or (45°49'30.7"N 4°50'58.4"E, France). The vadose zone was about 10 m deep. Both
101 of the saturated and unsaturated zones were contaminated by HCs as the consequence of
102 spills in the 1940's. From the surface, there was a first layer of embankments, then a silt
103 layer, and a sand one with 1.0, 0.3 and 4 m thicknesses, respectively. The latter was
104 contaminated by HCs up to 12000 mg.kg⁻¹. The microbial activity and nitrogen content (<0.5
105 gN.kg⁻¹) in soil were low.

106 **For lab studies**, soil samples were collected from the contaminated site at depths from 1 to 4
107 m below the ground surface (mbgs). Before being used, the HC contaminated soil was sieved
108 to remove the coarser fraction (> 1 cm), then it was mechanically homogenized and its main
109 physicochemical properties were evaluated. Particle size distribution was determined by
110 sieving [39]; the D₁₀ and D₉₀ of the collected fraction were 168 and 2040 μm, respectively.
111 D₁₀ and D₉₀ correspond to the 10th and 90th percentile of grain size distribution, respectively.
112 The soil permeability was 267 μm² **as measured using the constant head technique** [40]. The
113 soil porosity was 30.6% as measured by weighing a soil column before and after filling it with
114 water to determine its porous volume (PV) [41]. The measured pH of the soil was 9 (multi-
115 parameter analyzer Consort C862), using a 1/5w soil/deionized water ratio stirred for 1 h
116 [42]. The carbonates content of the soil was 4.5% **as measured by volumetric measurement**
117 **of CO₂ formed during acidic dissolution** [43]. The soil was hydrophilic, considering the
118 measured contact angle at the air/water/soil interface, **using the modified sessile method**
119 [44], which was 30°. The initial water content of the soil was 1%w as measured by the Karl

120 Fischer method [45]. Soil moisture content was determined in triplicates. Approximately 5 g
121 of sample were weighted before and after drying in an oven at 105 °C overnight (at least 16
122 h). Soil relative humidity was then calculated by weight difference [46]. Typically, the
123 average C10-40 semi-volatile and C5-C11 volatile total petroleum hydrocarbons (TPH)
124 indices measured in the soil were 3000 ± 324 and 44 ± 5 mg.kg⁻¹, respectively. Sums of 16
125 US PAH and BTEX concentrations were 20.0 ± 4.8 and 5.000 ± 0.003 mg.kg⁻¹, respectively.
126 Total nitrogen was measured using Total Nitrogen test kits (Merck) extractable phosphorous
127 (orthophosphates) was measured by the Olsen method [47].

128 2.2. Chemicals and reagents

129 The zwitterionic Lauryl Betaine (LB, 40%w, EOC) surfactant was used to make foam, as
130 previously reported [25,26,38]. Hydrogen peroxide (35%w, Acros Organics) and iron(II)
131 sulfate (FeSO₄.7H₂O, Fisher Scientific) were used to form the Fenton reagent. Sulfuric acid
132 (98%) was provided by Merck. Analytical reagents were ammonium thiocyanates (98%,
133 Prolabo) and hydrochloric acid (37%, VWR). Ammonium nitrate (>98%) and potassium
134 phosphate (>98%) were provided by Acros Organics. Magnesium sulfate (MgSO₄.7H₂O,
135 >99%), calcium chloride (>99%), ammonium chloride (>99.8%) and ammonium sulfate
136 (>99%) were provided by Merck. Sodium chloride (>99.9%) was provided by VWR. For field-
137 test, LB 40 %w, hydrogen peroxide (35%, Quaron), iron(II) sulfate heptahydrate (85%, UAB)
138 and sulfuric acid (37%, Ardea) were used.

139 The FR was prepared in a 1:5 ratio of iron(II) sulphate to hydrogen peroxide, because it is
140 stated in literature that the optimal H₂O₂/Fe ratio varies between 5 and 25 [17,48–51]. An
141 excess of iron causes an unproductive consumption of hydroxyl radicals and undesirable side
142 reactions, which increase the scavenging of hydroxyl radicals [52]. The concentration of FR

143 delivered was $9 \text{ g.kg}_{\text{soil}}^{-1}$, corresponding to concentrations of 4.4%w and 0.9%w for H_2O_2 and
144 FeSO_4 , respectively. The oxidant dose was estimated from the stoichiometric molar ratio
145 (SMR) between H_2O_2 and dodecane, considering the latter as being representative of the HC
146 contamination of the soil [53]. Since the low pH required for conventional Fenton oxidation
147 clean-up is of major importance, concentrated H_2SO_4 was added to the FR solutions to
148 decrease the pH of the injected solutions to 3, which in turn prevents strong precipitation of
149 Fe^{3+} [6,54].

150 2.3. Biological reagents

151 Based on an analysis of total N and extractable P amounts in the soil, the BS solution was
152 made of $(\text{NH}_4)_2\text{HPO}_4$ and K_2SO_4 , at 3.27 and 1.7 g.l^{-1} , in order to maintain a C:N:P ratio close
153 to 100:10:1. The BA solution was prepared using the same concentrations of N and P as in
154 the BS solution. Yet, the micro-organisms developed in a continuous reactor were added at a
155 colony forming unit (CFU) concentration of $(3.7 \pm 1.1) \times 10^7 \text{ CFU.ml}^{-1}$. The microbial
156 development was performed for 1 month in an aerated Continuous Stirred Tank Reactor
157 (CSTR) of 4.2 l at 293 K, as described previously [55]. The initial inoculum for the CSTR was a
158 mixed culture from different biological batch experiments. The batch experiments aimed at
159 testing and selecting indigenous bacteria that were present in the soil of the contaminated
160 site, regarding their ability to use the pure phase of HCs as a carbon source in presence of
161 high LB concentrations. Likewise, HCs from the contaminated site and LB were the only
162 carbon sources in the CSTR. The pure HC phase was injected in the reactor through a syringe
163 pump at a flow rate of 4.8 ml.d^{-1} . The nutrient feeding solution was made of $1 \text{ g.l}^{-1} \text{ NH}_4\text{NO}_3$,
164 0.05% LB, $0.1 \text{ g.l}^{-1} \text{ MgSO}_4$, $0.01 \text{ g.l}^{-1} \text{ CaCl}_2$, $0.4 \text{ g.l}^{-1} \text{ KH}_2\text{PO}_4$, $1.775 \text{ g.l}^{-1} \text{ K}_2\text{HPO}_4$, 0.05 g NaCl , 0.5
165 $\text{mg.l}^{-1} \text{ FeSO}_4.7\text{H}_2\text{O}$. This solution was injected by a peristaltic pump to maintain a 3.4 d

166 hydraulic retention time. The CSTR was run for one month, in order to select micro-
167 organisms able to degrade HCs in presence of LB in these operating conditions.

168 2.4. Experimental set-up

169 2.4.1. Laboratory scale

170 2.4.1.1. Column and sandbox description

171 Foams were pre-generated in all column experiments using a vertical pre-column (5 cm long,
172 i.d. 32 mm) containing glass beads with diameters ranging from 100 to 300 μm . The
173 surfactant solution and the gas were mixed just before the pre-column through a plastic-T.
174 The outlet of the pre-column was connected to the inlet of the soil column. The soil column
175 was a glass column filled with 62 g of soil by three compacted layers of 1.5 cm (4.5 cm long,
176 i.d. 3.2 cm). The soil sample set up used metallic grids. The column was set horizontally to
177 better mimic injection in field conditions. Syringe pumps, flow-meter and pressure sensor
178 were the same as those used in 2D-experiments.

179 The experimental set-up used for fluids injection in 2D-sandboxes is shown in Fig. 1. The soil
180 was packed in a PMMA sandbox (i.d.: 25 cm wide, 2 cm thick, 18 cm high). PMMA was
181 selected due to its transparency and chemical resistance. The front face was removable
182 using screws and gasket. The soil was compacted using a mallet while filling. Top lid and
183 gasket were then tightly held using clamps to ensure perfect sealing. All of the experiments
184 were conducted under unsaturated conditions. Foam was pre-generated using a 9 cm pre-
185 column (i.d. 18 mm) containing a non-contaminated soil particles with diameters ranging
186 from 244 to 1113 μm . For the experiments using foam, fluids were injected using a
187 homemade vertical plastic sleeved grouting pipe (SP) inserted into the soil. The SP carried a
188 rubber sleeve covering two opposed injection holes (see Fig. 1) from where fluids exited. An

189 epoxy resin plug prevented the injected fluids from rising inside the SP. The inlet of the SP
190 was connected to the outlet of the pre-column. The SP was used to get closer to the
191 injection tool used in the field-test (see section 2.3.2). Syringe pumps, flow-meter and
192 pressure sensor were like in Bouzid [26].

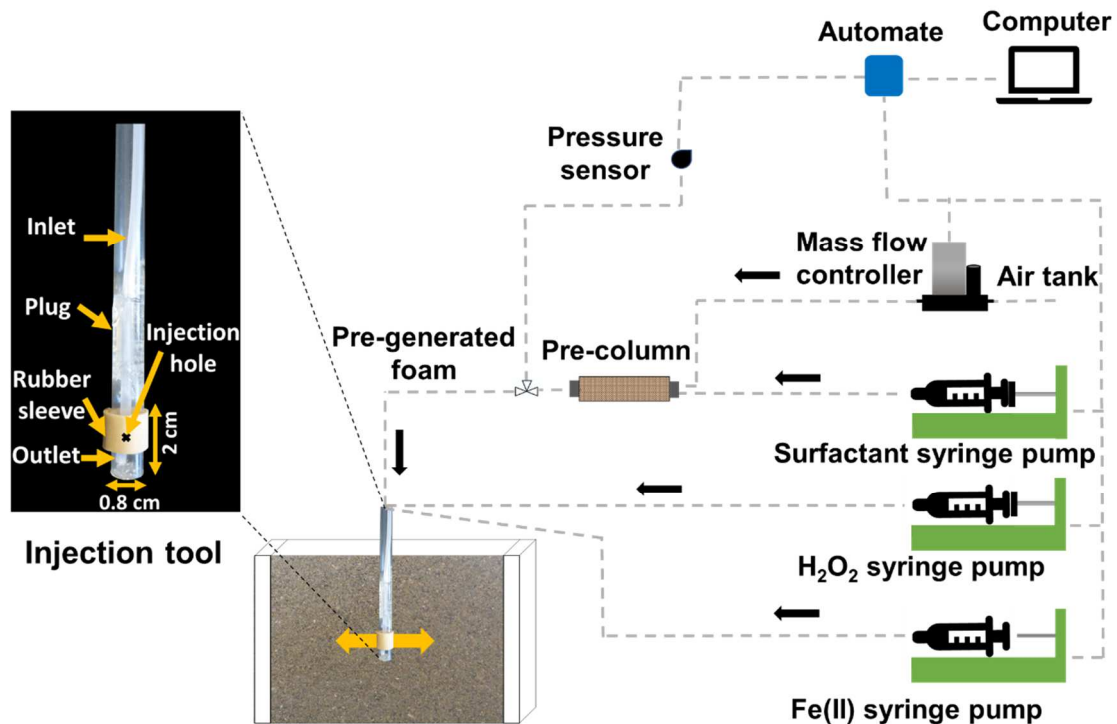


Figure 1. Experimental set-up used for fluids injections in 2D-experiments.

193 **2.4.1.2. Injection procedures**

194 The injection procedures were similar for all the experiments with foam. First, a pre-
195 generated foam was injected into the soil. The foam was made using a 4% LB solution and
196 had a quality factor (FQ) of 90%. Then FR were injected in a liquid form, with a low flow-rate,
197 in order to flow with a piston-like effect through the water network of foam [26]. Then, to

198 study the combination of treatments, biological reagents (nutrients and micro-organisms)
199 were injected in liquid form after 15 h, since the chemical oxidation was achieved within 3 h.

200 Different foam-based remediation strategies were assessed in column: (i) Fenton/natural
201 attenuation (F/NA), (ii) Fenton/biostimulation (F/BS) and (iii) Fenton/bioaugmentation
202 (F/BA). Before each combined treatment, the surfactant solution and gas were injected at
203 flow rates of 0.355 and 3.2 ml.min⁻¹, respectively, during 1 h, to obtain a homogeneous foam
204 at the outlet of the pre-column. Then, the outlet of the pre-column was connected to the
205 inlet of the soil column. Once the foam filled the column, 2 PV of H₂O₂ and of Fe²⁺ solutions
206 were directly injected into the soil column by two syringe pumps at flow rates of 0.4 ml.min⁻¹
207 ¹, during 64 min. The relative soil humidity after this injection was 5 ± 1%. Finally, for
208 combined treatments with BS or BA, 2 PV of BS or BA solutions were directly injected into
209 the soil column with a syringe pump at a flow rate of 0.4 ml.min⁻¹. The relative humidity
210 after these injections was 9.4 ± 0.5%. Effluent samples were taken for plate count analysis to
211 determine the percent of viable cells that were transported through the column. For each
212 remediation strategy, some columns were directly analyzed whereas others were closed
213 with stoppers and maintained at 298 K for 40 d before being analyzed.

214 For sandboxes experiments, two FR delivery methods were compared. FR were delivered
215 either directly as solutions in water (W-FR) as a reference method or as these solutions
216 delivered after foam injection (F-FR) through the same opening. Experiments were
217 duplicated to ensure repeatability. For all the experiments, the FR were prepared *in situ* by
218 alternatively injecting acidified (pH 3) iron(II) and H₂O₂ solutions, using the SP. For W-FR
219 experiments, 60 ml of amendment solutions could be injected (at a 8 ml.min⁻¹ flow rate)
220 until the bottom of the sandbox was reached. For F-FR experiments, pre-generated foam

221 was first injected. After the foam filled the edge of the sandbox, the FR-solutions were
 222 alternatively injected to replace the surfactant solution held in the foam lamellae network.
 223 In order to deliver the required dose, three oxidant injection cycles separated by 1 h reaction
 224 time each were carried out. For each cycle, the FR produced *in situ* had a concentration of
 225 4.4%w. This was carried out by injecting alternatively acidified H₂O₂ (4.4%w) and FeSO₄
 226 (0.9%w) solutions at a 2 ml.min⁻¹ flow rate. This injection method was chosen to avoid the
 227 use of very concentrated H₂O₂ solutions. Indeed, for F-FR experiment, to deliver the same
 228 amounts of oxidant into the soil, the final water saturation (33%) was considered, to
 229 calculate FR-concentrations which were delivered. Thus, FR-concentration (H₂O₂ and Fe²⁺
 230 solutions) was 3-times higher (13.3%w), to deliver the same amount of FR than in the W-FR
 231 experiments (4.4%w). The volume of FR injected was the one required to push the surfactant
 232 solution out the foam's water network. This was achieved by calculating the porous volume
 233 of the soil filled with foam using, the ImageJ software [56] and the known water saturation
 234 (33%) in that zone. The calculated volume of FR-solution was 0.3 PV for each cycle. A
 235 pressure gradient limit was set at 0.1 MPa.m⁻¹ for injection to avoid soil fracturing or heaving
 236 in field conditions [57].

237 To quantify the oxidant distribution efficiency, an isotropic distribution factor, (*I_f*,
 238 dimensionless) was calculated according to eq.2 [25]. The *I_f* is the iron concentration-
 239 weighted ratio of its propagation distances in the vertical and horizontal directions from the
 240 injection point, which allows the comparison of delivery and sweeping efficiency between
 241 experiments.

$$242 \quad I_f = \frac{\sum dv^- Cv^- / \sum dv^+ Cv^+}{\sum |dh| Ch / \sum |dv| Cv} \quad (2)$$

243 where d and C are the propagation distance and the iron concentration at a given distance
244 from the injection point, respectively. The indexes v and h represent the vertical and the
245 horizontal directions, respectively, and the + or – signs indicate the upper and lower or right
246 and left direction for the vertical and horizontal distances, respectively. The optimal I_f value
247 would be 1, representing an isotropic reagents distribution, and meaning that the horizontal
248 and vertical distribution of the oxidant are equal. In contrast, high or low I_f -values indicate an
249 anisotropic distribution of reagents around the injection point.

250 2.4.2. Pilot scale

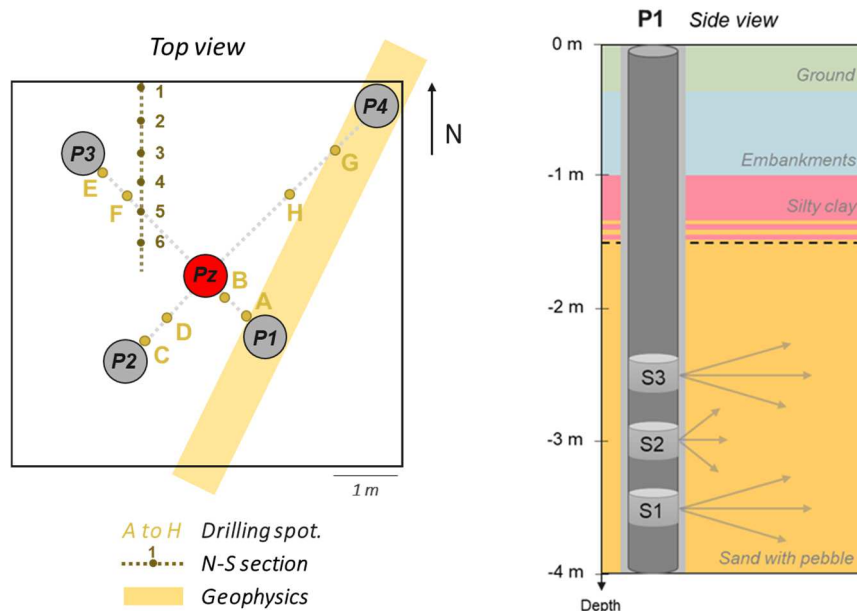
251 The tailored field injection procedure was set up using the soil lab studies. The key points
252 were the use of sleeved tubing systems and a three-steps injections using a pre-generated
253 foam, FR and BS or BA solutions. The goals were to assess fluids injectability and treatments
254 efficiency in field conditions.

255 Four injection wells (P1 to P4) were PVC pipes (d.: 7.6 cm). They were set down to 4 mbgs,
256 with 1 cm openings (S1 to S3) at 2.5, 3 and 3.5 mbgs locked with rubber bands (Fig. 2 right)
257 and surrounded by a cement frame (cement/water: 0.26). SP allows a better depth
258 selectivity during the injection. The four injection wells were set in a spiral arrangement
259 around a central control well (Pz, Fig. 2 left), to better assess the foam-based method ROI.

260 The control well was set down to 6 mbgs in the sandy layer and perforated from 2 to 6 mbgs.

261 To assess the HC degradation rates, drillings were performed on the treated area, to collect
262 soil samples after 10 and 110 d. Sampling was realized as shown in Fig. 2 (left). Drilled
263 samples were obtained from 3 to 4 mbgs at spots A to G. Besides, samples at spots 1 to 6
264 were collected at 3 mbgs using a power shovel. Average contaminant concentrations in the

265 plot were determined using P1 to P4 drilling cuts, recovered from 2 to 6 mbgs. The lithology
 266 along P1 to P4 is shown in Fig. 2. The injections were performed in the sand layer.



267

Figure 2. Left: injection and control wells. Sampling plan: drilling along N-S section and local sampling points A to H. Geophysical monitoring along yellow line. Right: side view of the SP and lithological section of the plot.

268 **2.4.2.1. Injection procedures**

269 For each step, successive injections through openings were performed using a stainless-steel
 270 injection pipe (Petrometalic) equipped with two packers separated by 0.35 m. Packers were
 271 placed on each side of the opening and inflated with water. Then, the free space between
 272 the packers (volume: 1.6 l) was isolated from the rest of the pipe and was filled with foam,
 273 then with either liquid oxidant or BA/BS solutions using a $1 \text{ m}^3 \cdot \text{h}^{-1}$ volumetric rate peristaltic
 274 pump. The carried foam, FR and BA/BS solutions were prepared on-site: 0.024 m^3 of LB 40%
 275 were diluted in 0.6 m^3 of water to have a 4% solution; 10 kg of iron sulfate were suspended

276 in 0.55 m³ of water, to have a 1.5% FeSO₄ solution, and acidified to pH 5 with H₂SO₄ (37%);
277 0.06 m³ of H₂O₂ were diluted in 0.54 m³ of water to have a 3.5 % solution. BS and BA
278 solutions were prepared in a 0.4 m³ stirred tank.

279 Works were carried out in four steps. First, the cement shells around SPs were broken down
280 using high pressured water. During this step, flow rate, pressure and injected water volume
281 were monitored to avoid ground fracturing. Stop values were set to 3.6 m³.h⁻¹, 1 MPa and
282 0.15 m³ per opening. After the breakdown of the cement shells, the injection pressure
283 sharply dropped from 1 to 0.1 MPa, while flow rate increased, suggesting that water flowed
284 into the soil. At this point the water injection was stopped. Then, the LB solution was loaded
285 in a 0.025 m³ foam generator (GS-30, Netzone Consult). The pre-generated foam (FQ: 80%)
286 made by the foam generator was then injected using the stainless-steel injection pipe at a
287 flow rate of 0.2 m³.h⁻¹. After the foam injection, FR solutions were injected in two steps to
288 prevent an exothermic reaction in the pipes: 0.1 m³ of 1.5 % iron sulfate solution were
289 injected, followed by 0.05 m³ of 4% H₂O₂ solution. 0.2 m³ of FR solution were injected in
290 each P1 and P2 opening, 0.5 m³ in each P3 and P4 opening, with a flow rate of 0.9 m³.h⁻¹ and
291 an average pressure of 0.5 MPa.

292 Finally, biological post-treatments were applied, considering F/BS and F/BA carried out in P1
293 and P2, respectively. Based on a N and P content of the soil, the BS solution was 0.75 g.l⁻¹
294 KH₂PO₄, 0.5 g.l⁻¹ KH₂PO₄, 5 g.l⁻¹ (NH₄)₂SO₄, 1.25 g.l⁻¹ NH₄Cl, 0.31 g.l⁻¹ (NH₄)₂HPO₄, 1.25 g.l⁻¹
295 NH₄NO₃. The BA solution was prepared using the same N and P concentrations, and the
296 addition of the microorganisms developed in the 0.4 m³ stirred batch reactor for 12 d. The
297 temperature ranged between 286 and 292 K during the development. The initial viable cells
298 concentration was 8.5 10⁸ cfu.ml⁻¹. The growth medium was composed by 0.01% LB, 0.5 g.l⁻¹

299 $(\text{NH}_4)_2\text{HPO}_4$, 0.5 g.l^{-1} HC pure phase, 0.25 g.l^{-1} of NAPL, 0.25 g.l^{-1} of diesel previously altered
300 by a Fenton reaction. After a 12 d growth, the final viable cell concentration was 2.10^8
301 CFU.ml^{-1} . For the F/BS and F/BA treatments, 0.1 m^3 of solutions were injected through each
302 SP opening using a peristaltic pump ($1 \text{ m}^3.\text{h}^{-1}$, 0.2 MPa).

303 2.4.2.2. Geophysical monitoring

304 One of the main advantages of using ERT is its ability to provide spatial information about
305 the subsurface in a minimally invasive manner at a quite **good** resolution. In addition, it
306 allows the collection of a suite of continuous datasets at the same location as a function of
307 time that can highlight changes in the system [58]. Foam injections in P1 and P4, and iron(II)
308 solution injection in P1 wells were monitored using 2D ERT. A 36 electrodes electrical profile
309 line was disposed along the injection wells P1 and P4 (Fig. 2). The geoelectrical data were
310 collected using a system of multi-electrodes measurement (SYSCAL R1 and switch 72, Iris
311 instruments). The system was equipped with a resistivity meter connected to a cable with
312 multiple outlets connected to the 36 stainless-steel electrodes. They were set in the ground
313 at regular intervals of 0.7 m to allow a depth investigation of about 4.5 m. The electrical
314 measurements were taken according to a Wenner-Schlumberger configuration sequence
315 along a rectilinear profile. Acquired data were then automatically filtered, to eliminate
316 negative values and values with $\text{s.d.} > 1\%$. Measurements after inversion using the Res2DInv
317 software (Geotomo) were then represented in the form of a pseudo-view of the repartition
318 of apparent resistivity vs. depth [59]. Finally, the local resistivity data were analyzed with the
319 software Surfer (Golden Software) to get a deeper analysis of the local resistivity changes in
320 the soil during the injection steps.

321 2.5. Analytical methods

322 2.5.1. Hydrocarbons extraction and analysis

323 Two methods were compared to remove HC in sandboxes experiments: the first one used
324 the photo-ionization detection (PID) method, for volatile organic compounds (VOCs) and the
325 second one used GC/FID and GC/MS for C10-C40 and C5-C11 TPH measurements,
326 respectively. For both methods, HC concentrations in sandboxes were locally measured, to
327 create a map of HC removal rates, 24 h after the FR injection. For the first method, HC
328 concentrations were determined with a Photo-Ionization Detector (PID, Tiger Ion Science)
329 using isobutylene as a calibration gas with a 1 ppb detection limit. The linear range of
330 detection was up to 800 ppm. Recovery upon soil spiking with pure phase of the HCs
331 collected from the site was 97.3%, while the sensitivity of a typical calibration curve was
332 0.0157 ($R^2 = 0.9999$). The PID method was tested because of its rapidity, low cost, the
333 number of samples and the repetitions that can be carried out. Before the PID
334 measurements, the soil was thoroughly sampled after the removal of the sandbox front face.
335 For each sampling, 5 g of soil were transferred into a glass vial, mixed, and let to rest for 5
336 min before the measurement of the gas phase. The effect of water and surfactant
337 concentrations on the VOC concentrations measured were considered using calibration
338 curves. C10-C40 TPH were obtained according to the NF EN ISO 9377-2 analysis as follows:
339 50 μ l of the extracts were analyzed using GC/FID (Thermo Trace 1300, VF Select Mineral Oil
340 15 m capillary column with 0.32 mm i.d., film diameter 0.10 μ m). Hydrogen was used as a
341 carrier gas. The initial oven temperature was 308 K for 3 min and increased by 313 K.min⁻¹
342 until it reached 593 K. For field soil samples, C10-C40 TPH indices and the sum of 16 US PAHs
343 were performed following the NF EN ISO 16703 and NF ISO 18287 standards, and
344 quantification limits were 15 and 0.8 mg.kg⁻¹ for TPH and PAH, respectively. Variability was
345 40 and 28% for TPH and PAH concentrations, respectively. C5-C11 TPH were obtained

346 according to the XPT 90-124-analysis as follows: 1 ml of the sample vapor phase were
347 analyzed using GC/MS (Thermo Trace DSQ, head space). Helium was used as a carrier gas.
348 The initial oven temperature was 313 K for 5 min and then increased by 288 K.min⁻¹ until it
349 reached 423 K. The TPH quantifications were carried out by external calibration using
350 certified standards.

351 2.5.2. Iron determination

352 Iron concentrations (g.kg⁻¹) in sandboxes were determined as follows: first, 20 g of sampled
353 soil across the cell were transferred in glass flasks with 50 ml deionized water and 2 ml
354 hydrochloric acid (6 mol.l⁻¹). Then, the flasks were shaken using an orbital shaker for 30 min
355 to extract iron into the water phase. Then, the samples were filtered through Whatman
356 paper and 1 ml NH₄SCN (1 mol.l⁻¹) and 1 ml H₂O₂ were added to filtrates to form the
357 Fe(SCN)²⁺ complex. Finally, the brown complex was quantified by UV-vis spectrometry
358 (Agilent Cary 100) at 475 nm [60].

359 2.5.3. Respiration assays

360 Oxygen uptake was monitored during degradation using an Oxitop[®] system [61]. 40 g of
361 fresh sample were placed in Oxitop[®] jars and incubated at 298 K. Soil respiration (SR) was
362 calculated according to the eq. 3.

$$363 \quad SR = \frac{M(O_2)}{R.T} \cdot \frac{V_g}{M_S} \cdot \Delta P(O_2) \quad (3)$$

364 where SR is the soil respiration (mg O₂ g⁻¹ DW), M(O₂) is the molar mass of oxygen (mg.mol⁻¹)
365 ¹), V_g is the free gas volume (m³), ΔP(O₂) is the pressure difference (hPa), R is the gas
366 constant (m³.Pa.K⁻¹.mol⁻¹), T is the measuring temperature (K) and M_S is the soil dry mass (g
367 DW).

368 To compare the influence of different treatments on the respirometry, SR ratio was

369 calculated after 10 d of treatment:

$$370 \quad R = \frac{SR_X}{SR_{NA}} \quad (4)$$

371 where SR_X and SR_{NA} are the SR after a given treatment and after the Fenton treatment
372 alone, respectively.

373 2.5.4. Microbial plate counts

374 Viable cells were extracted from the soil by mixing 5 g of soil with 20 ml of a solution
375 containing NaCl (9 g.l⁻¹) and K₂HPO₄ (3.5 g.l⁻¹) at pH 7.0 [62]. These samples were then mixed
376 for 30 s using a vortex mixer before a further dilution in the NaCl and K₂HPO₄ solution [63].
377 Dilutions from 10⁻¹ to 10⁻⁶ were then performed in series and 0.1 ml of each dilution was
378 plated onto a solid plate count agar medium and incubated for 72 h at 303 K. The results are
379 expressed as CFU per g.

380 3. Results

381 3.1 Lab-scale

382 3.1.1. Comparison of methods for reagents delivery and oxidation efficiency

383 The deliveries of FR solutions into the soil considering either their direct injection or after
384 foam injection were compared. The distribution of FR and C10-C40 TPH removal rates
385 obtained after oxidation are shown in Figure 3. The removal rates obtained after oxidation
386 for both methods using the PID are summarized in Fig S1.

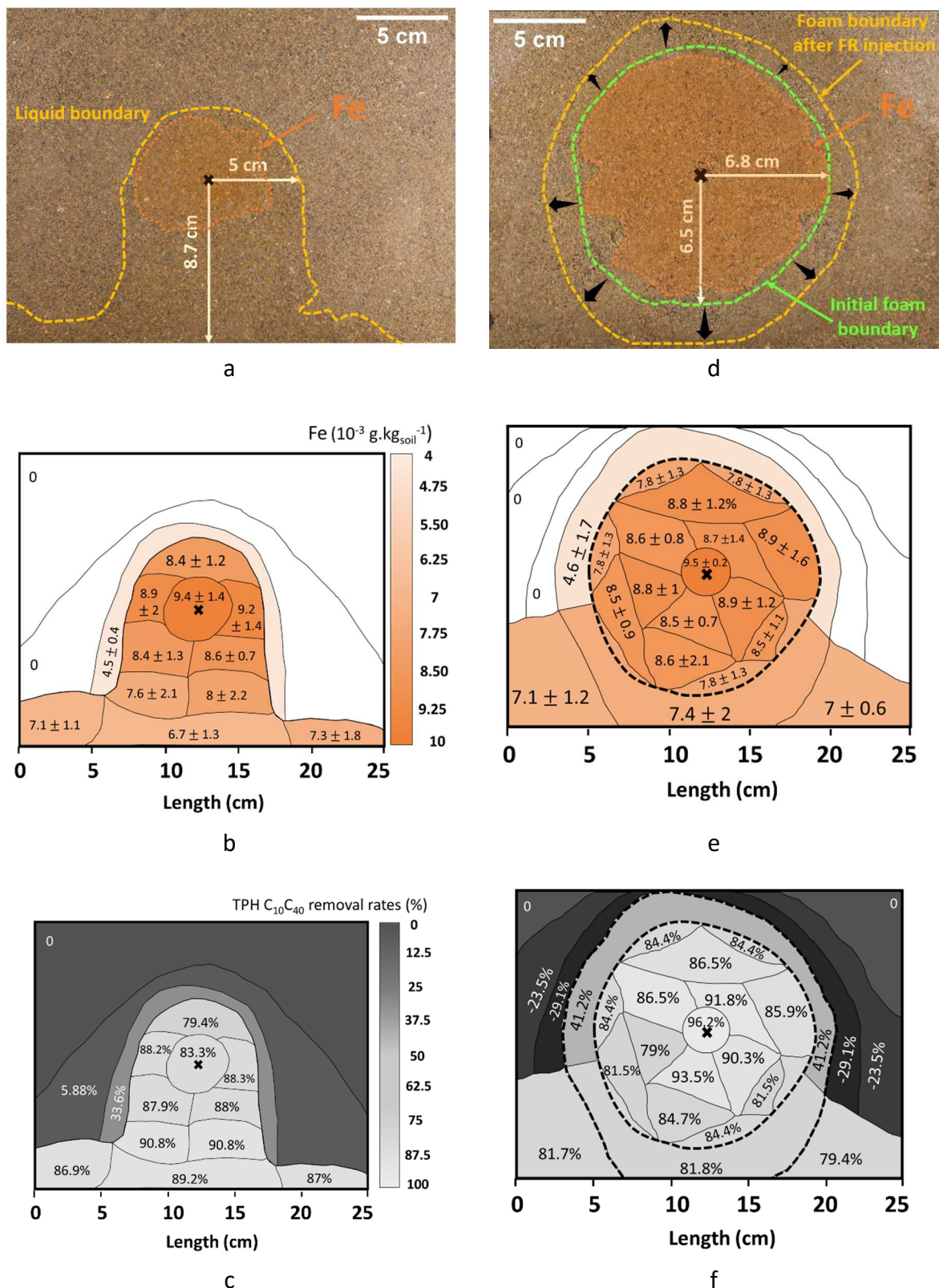


Figure 3. Top: FR visual distribution (a) after direct injection of the solutions (W-FR) and (d) using the foam-based method (F-FR). Middle and bottom: maps of Fe distribution and C₁₀-C₄₀ TPH removal rates, respectively: (b,c) after direct injection of the solutions and

(e,f) using the foam-based method. Black cross indicates the injection point. Fe concentrations varied from 0 (white) to 10^{-3} g.kg_{soil}⁻¹ (dark orange). Standard deviations for C10-C40 TPH indices ranged between 0.5 and 2%.

387

388 The propagation of FR solutions resulting from their direct injection (Fig. 3a), was dominated
389 by gravity and solutions accumulated at the bottom of the sandbox. In contrast to
390 hydrophobic coal tar contaminated soils, the contaminated soil was initially hydrophilic and
391 solutions also propagated above the injection point because of some capillary suction [28].
392 Visually, the FR propagation within the contacted area was hindered, since the brown color
393 of the Fe³⁺ accumulated preferentially around the injection point (see the orange dashed
394 lines in Fig. 3a). This observation was confirmed both by the low I_f-value (0.58 ± 0.03) and by
395 the Fe distribution map (Fig. 3c), where the highest Fe concentrations were close to the
396 injection point. Fe concentrations varied 2-times between the lowest and the highest ones
397 within the swept zone. The slight difference of Fe concentrations could be explained by local
398 soil heterogeneity and preferential flows. Fig. 3c presents the C10-C40 TPH removal rates
399 map across the sandbox for the direct injection of FR. The removal rates were high in the
400 contacted areas thanks to acidification to pH 3 and varied between 79.4 and 90.8% above
401 and below the injection point, respectively [64–66]. Indeed, preliminary oxidation tests
402 carried out without the acidification of the FR revealed that the HC removal rates did not
403 exceed 40%, as previously reported [67,68]. In addition, the precipitation of Fe³⁺ leads to the
404 plugging of the injection pipes and the soil pores, which resulted in poor FR solutions
405 injectability. The C5-C11 TPH removal rates measured after oxidation were 100% for all the
406 contacted areas. C10-C40 TPH removal rates were similar to those calculated using the fast
407 and cheaper PID method (see Fig. S1a), confirming that the latter can be considered as a

408 reliable method to monitor the TPH removal rates. Nevertheless, the ROI of the FR solution
409 needs to be improved, in order to decrease the treatment costs and the uncertainties
410 associated to poor reagents delivery.

411 Experimental documents reporting the performances of the foam-based method are shown
412 in Fig. 3d-f. The pre-generated foam flowed quite isotropically around the injection point
413 (green dashed lines in Fig. 3d) and with an improved ROI, as previously reported [25–27,69].

414 In contrast to solutions, foam propagation is mainly controlled by its high viscosity, that
415 overcomes gravity [25]. In order to maximize the selectivity of the oxidation, the previously
416 developed foam-based method was applied [25,26,28]. The FR was made *in situ* after foam
417 injection (see green and yellow lines in Fig. 3d). As shown in Fig. 3d, H₂O₂ and FeSO₄ were
418 successfully mixed *in situ* to produce the FR, as shown by the light brown color that
419 developed quite homogeneously within the foam. The FR injection led to the expansion of
420 the foam's initial volume by 0.7-times. This increase is explained by three phenomena: first,
421 surfactant production during HC oxidation [7], second, O₂ production from the
422 disproportionation reaction of H₂O₂, and third, gas production during HC mineralization.

423 During the three injection cycles of FR, the highest allowed pressure gradient (0.1 MPa.m⁻¹)
424 was recorded at the launch because at this moment, HC concentration was the highest one.

425 During the next two cycles, the injection pressure gradient did not exceed 0.07 and 0.04
426 MPa.m⁻¹ for the second and third cycles, respectively. Both of these lower pressures are

427 explained by the decrease of HC concentrations in the treated zone. Fig. 3e shows the Fe-
428 concentration map in the sandbox when using the foam-based method. As seen for the
429 propagation of FR solutions when they are directly injected, the highest Fe-concentration
430 was obtained near the injection point. However, they varied only 1.2-times between the
431 lowest and highest values within the zone filled with foam. Horizontal and vertical oxidant-

432 distributions were roughly equal as demonstrated by the I_f -value amounting to 0.95 ± 0.04
433 which is close to the optimal value, in contrast to W-FR experiment. Fig. 3f presents the map
434 of C10-C40 TPH removal rates in the sandbox. They were better than for the W-FR method
435 and greater than 79% within the zone filled with foam. After a 24 h reaction time, the soil pH
436 only reached 4, showing the persistence of the acidification in the area contacted by foam.
437 However, it is worth mentioning that about 25% were displaced outside the foam zone
438 during the foam injection phase, because of its strong viscosity [26,30,32,36]. This explains
439 some locally negative C10-C40 TPH removal rates obtained in the vicinity of the front line of
440 foam. The highest TPH removal rate was obtained near the injection point (96.2%), where
441 the highest FR-concentration was observed too. Lower TPH removal rates (~81%) were also
442 observed at the bottom of the cell, outside the foam boundary (Fig. 3f). It confirms that
443 some oxidant was expelled outside the foam, probably during the second and third injection
444 cycles; this is also explained by a less selective oxidation reaction due to mixing with some
445 surfactant, pushed away by the oxidant [25,26]. Once again, C5-C11 TPH were completely
446 removed inside the foam filled region, whereas C10-C40 TPH removal rates were similar to
447 those calculated using the PID (see Fig. S1b). Yet, when considering the global TPH removal
448 in the whole sandbox, the F-FR method was 20% more efficient than the W-FR one. TPH
449 removal kinetics were pseudo-first-order. Apparent rate constants were 2.43 ± 0.1 and 2.04
450 $\pm 0.05 \text{ h}^{-1}$ for W-FR and F-FR, respectively. The lower value for F-FR is explained by the
451 presence of 13% of the surfactant initially injected after FR injection, as previously explained
452 [28]. This remaining surfactant resulted from adsorption at interfaces and by-passing
453 phenomena in the porous medium. Hence, the main conclusion here is that the ISCO
454 treatment was much more controlled and effective when using foam. As ISCO lowers the HC-
455 concentrations and improves the bioavailability of the parent compounds, facilitating

456 indigenous bacterial activity, their combination was studied in non-acidified condition as
457 follows.

458 3.1.2. Combined treatments

459 To reduce the treatment cost and the acidification impacts, the coupling of ISCO, without
460 acidification, with biological treatments as a polishing step for the removal of the residual
461 contaminant mass, was assessed. Three main aspects of this coupling were studied: (i) the
462 influence of the Fenton reaction on the microorganisms concentration in soil, microbial
463 activity and pollutant degradation during the natural attenuation (F/NA); (ii) the influence of
464 the addition of nutrients, i.e. biostimulation, (F/BS) on the microbial growth and activity in
465 soil; (iii) the influence of the addition of microorganisms, i.e. bioaugmentation, selected and
466 developed in a continuous reactor on the HC degradation activity in the soil.

467 Figure 4A shows the concentration of viable cells (CFU.g⁻¹ of dry soil) before and after each
468 treatment. After the oxidation treatment, the CFU in soil was reduced by two orders of
469 magnitudes. Besides, BA caused an increase in the number of viable microorganisms in the
470 soil immediately after the injection. Consequently, the microbial injection allowed the soil to
471 reach a CFU value which was similar to those measured before the chemical oxidation.

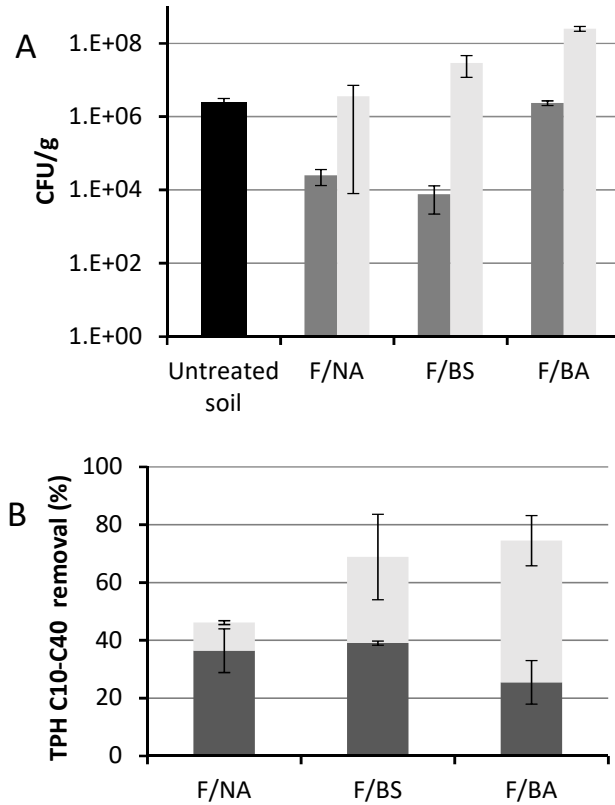


Figure 4. A) Colony forming units (CFU) concentrations for the untreated soil (■) and after applying the combined treatments in soil immediately after injection (■) and 40 d after injection (▒). B) HC removal after applying the coupled treatments in soil columns immediately after injection (■) and after 40 d of treatment (▒).

472 After 40 d, an increase by two order of magnitudes of the average of the number of viable
 473 cells was observed suggesting a possible rebound effect in the F/NA treatment, in agreement
 474 with [21]. Similarly, both of the BS and BA treatments allowed the CFU to increase by three
 475 and two orders of magnitudes, respectively. The enhanced microbial growth in the BS
 476 treatment is explained by a higher N and P availability, which can promote microbial
 477 development. Besides, the higher microbial growth observed after F/BS in relation to F/BA
 478 could be related to the higher initial amount of viable cells in the BA soil compared to the BS

479 one. This higher initial viable cells lead to a higher consumption of nutrients in F/BA soil
480 columns.

481 The results of respirometry experiments demonstrated that the oxygen consumption was
482 enhanced by BS and BA compared to NA after 10 d (Fig. S2). The difference in activity
483 between NA and BS can also be explained by the low nutrient content in the original soil and
484 the slightly lower amount of initial humidity in soil. Moreover, these results show that the
485 activity in the BA columns was higher than in the BS ones, because of a higher amount of
486 viable cells.

487 The overall HC removal after each combined treatment is shown in Figure 4B. After use of FR
488 treatment without acidification, HC removal was ranging from 25% to 40%. However, this
489 value was lower for the F/BA treatment. Indeed, even if HCs were mostly separated from it,
490 the BA solution still contained these compounds. Consequently, a notable amount of HCs
491 was injected into the columns (about 15% of the initial HC concentration), which explains the
492 decrease in the removal efficiency in this condition.

493 Forty days after the Fenton treatment, NA had increased the HC elimination by about 10%
494 while BS and BA treatments had increased it by 30% and 49% on average, respectively (i.e.
495 20% and 39% higher than NA). These results and the higher soil microbial activity observed
496 in these columns can result from the fact that F/BS and F/BA treatments produced higher
497 CFU values. This shows that the bacterial growth observed during these treatments was not
498 only connected to the HC biodegradation, but also to the consumption of natural organic
499 matter in soil and oxidation by-products. However even if in average F/BA treatment
500 allowed to reach higher removal than F/BS treatment, the results obtained are not
501 statistically different.

502 These results show that coupling Fenton and biological treatments after the foam injection is
503 effective, since Fenton-like reactions lead to oxidation products that are more soluble in
504 water and thus more bioavailable [17,70].

505 Furthermore, after the Fenton treatment, indigenous microorganisms continued to degrade
506 HCs in soil, and the addition of nutrients also boosted this phenomenon. Yet, by adding HC-
507 consuming microorganism selected and acclimated from the contaminated soil, the
508 treatment was more efficient than BS alone. Similar results were reported in more optimal
509 growth conditions for microorganisms [10,11,21]. Bajagain [12] also obtained a better HC
510 removal efficiency by spraying BA foaming solutions in a combined chemical
511 oxidation/biodegradation treatment. However, to the best of our knowledge, this is the first
512 time that a coupled chemical oxidation/biodegradation treatment was tested in a real
513 contaminated soil under unsaturated conditions after a foam injection.

514

515 3.2 Field-scale

516 3.2.1. Reagents injection

517 Figure 5 shows the foam aspects observed in the field during the different treatments
518 phases.



Figure 5. a: Surfactant foam after production at the output of the foam generator; b,c and d: resurgence in the central well (Pz) after injection in P1 of foam alone, iron sulfate solution and hydrogen peroxide solution, respectively.

519 Considering a soil porosity of 30%, 0.2 m³ of pregenerated foam (Fig. 5a) were injected in
 520 each opening of P1 and P2 wells to get a 0.5 m ROI. Foam resurgence in Pz (Fig. 5b) was
 521 observed after a 0.2 m³ injection in S1-P1, suggesting that, actually, the ROI would be about
 522 1 m. The structure of the resurging foam was very similar to the injected one.

523 Considering the distance between P1 and Pz and the resurgence time of the foam, its
 524 propagation rate was estimated at 3 m.h⁻¹. After a 0.1 m³ iron sulfate solution injection, a
 525 brown structured foam exited Pz (Fig 5c). Yet, after a 0.1 m³ of hydrogen peroxide injection,
 526 a less structured foam containing more gas quickly exited Pz (Fig. 5d). A sample of this foam
 527 was collected; 15 min later, its volume increased by 30% (Fig. S3). It confirmed that, because

528 of the reaction between H_2O_2 and the HC contaminated soil, a production of gas occurred, as
529 observed in part 3.1.1.

530 **3.2.2. Geophysical monitoring of the fluids propagation**

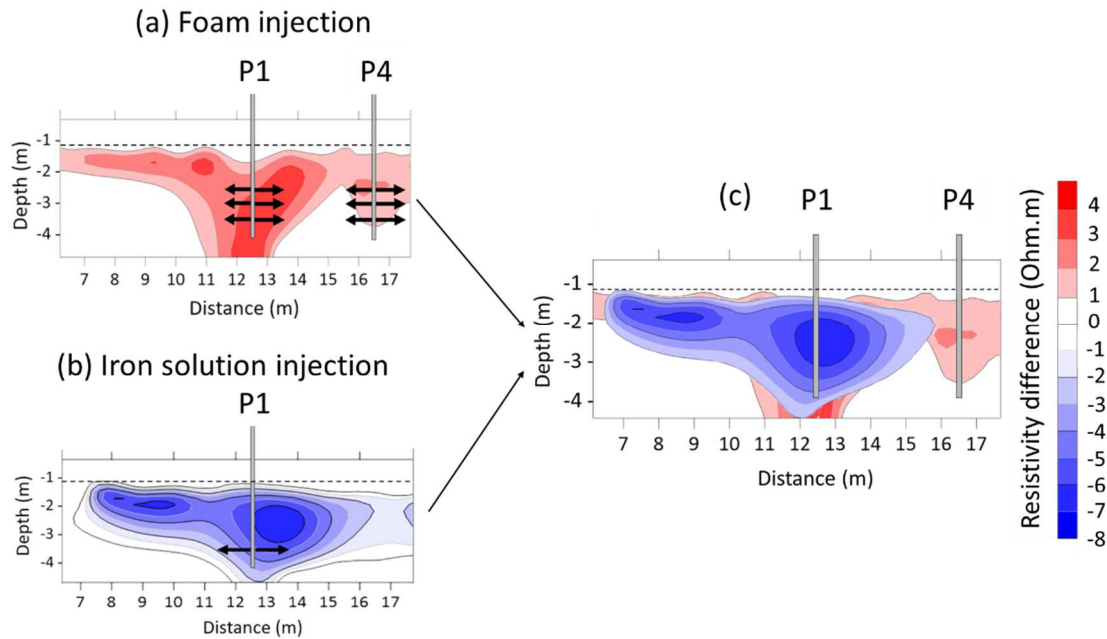


Figure 6. Changes in electrical resistivity after foam injections in P1 and P4 (a) and then after iron solution injection in P1 (b), and the combination of the two profiles (c).

531 Figure 6 shows differential ERT 2D profiles of the transect, where the foam and the iron
532 solution were injected (Fig. 2). The profiles were obtained by using a differential mapping of
533 local electrical resistivities between each step. The first reference state was the breakdown
534 of cement shell around the injection wells, then the second one was the injection of foam in
535 P1 and P4. Red and blue colors (positive and negative values, respectively) indicate an
536 increase and then a decrease of the soil electric resistivity after the successive injections of
537 foam and iron solution.

538 In fact, the electric resistivity of the soil is mainly controlled by the water saturation. Fig. 6a
539 represents foam injections in P1 and P4. A transient regime is firstly observable, where the
540 injected foam was destabilized by the presence of HCs [26,71]. At this moment, a weak foam
541 propagated beneath the low permeability silty-clay layer as shown by the significant
542 fingering. Then, a steady state was reached, where a viscous strong foam propagated with a
543 flat front. Thus, the soil became locally more electrically resistive. It is related to the
544 reduction of moisture and to the number of available electrical pathways through the water
545 films between gas bubbles [58,72]. The region swept by the foam exhibits a symmetry
546 around the injection wells with about 1 m ROI, as expected from the foam volume injected.
547 The day after, the injection of the iron solution in P1-S1 was also tracked. The differential
548 ERT profile and the combination of the foam/iron profiles are presented in Fig. 6c. Results
549 from the differential ERT profiles showed a good match for the propagation of foam and the
550 iron solution (Fig. 6 c). This suggests that the Fe solution successfully propagated through the
551 network of foam lamellae created into the soil.

552 3.2.3. Treatment efficiency assessment

553 The treatment efficiency was assessed considering injectability, C10-C40 TPH degradation
554 rates at 10 and 110 d, ROIs and the cost/benefit/risk balance.

555 Foam injectability using SP was relatively low. Three days were needed to inject 4.2 m³ of
556 pre-generated foam in a 10⁻⁴ m.s⁻¹ soil hydraulic conductivity. It corresponds to a flow rate of
557 0.175 m³.h⁻¹ for 8 h a day. It is lower than those reported by Portois [31], and it is explained
558 by the much higher hydraulic resistance of the injection tool used. Oxidant solutions
559 injectability was good, with a flow rate of 0.9 m³.h⁻¹, which is 5-times higher than the foam

560 flow rate. Resurgences of foam from Pz were observed throughout the oxidant injection. The
561 injectability of BA and BS solutions was also good.

562 A difficulty of the developed foam-based method would be to control the right propagation
563 of the solutions, since high injection rates can lead to foam fracturing and anisotropic
564 distribution of reagents. Yet, differential ERT images suggest that the F-FR method is quite
565 robust. Samples from 1 to 6 and A to H were drilled at 3 m deep along a N-S transect and
566 around P1 to P4 after 10 and 110 d of treatment, respectively (see Fig.2). HC concentrations
567 and degradation rates were quite changeable in the plot and measurement uncertainties
568 (~40%) were high (Table S1). HC concentrations along the N-S transect, after the Fenton
569 treatment, are shown in Figure 7.

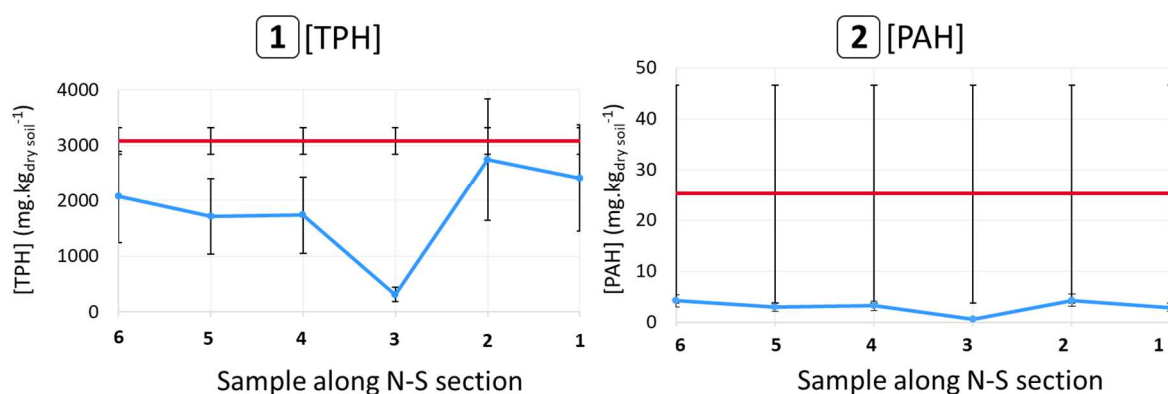


Figure 7. TPH C10-40 (1) and PAH (2) concentrations in soils along N-S section (see Fig. 2 for samples collection). Each sample was collected at 3 m deep, 10 d after Fenton reagent injection. Red lines show the average contaminants concentrations before treatment.

570 Despite large uncertainties observed for C10-40 TPH removal rates, contaminant
571 concentrations were clearly lower after treatments. Based on results in Fig. 7, ROI were

572 estimated to be from 1 to 3 m, in agreement with the differential ERT-profile obtained after
573 the injection of the iron solution (Fig. 6).

574 After 110 d, average C10-C40 TPH and PAH degradation rates (samples A to H) were $30 \pm$
575 28% and $68 \pm 25\%$, respectively. The highest TPH degradation rates, around $60 \pm 28\%$, were
576 obtained in B and D samples, suggesting further HC degradation by the biological post-
577 treatments applied in P1 and P2. This matches respirometric experiments performed 10 d
578 after the injections, which demonstrated an enhancement of the soil oxygen consumption
579 after BS and BA (R factor in B, C and D sampling amounted to 1.5, 2.5 and 1.5, respectively).
580 The overall moderate HC degradation rates of 30 % can be connected to the low acidification
581 of the injected FR. In this condition, the Fenton reaction is not strong enough, as previously
582 reported (see part 3.1.1).

583 Considering costs, the surfactant used to generate foam is twice more expensive than
584 oxygen peroxide. Yet, when the foam-based method is carried out, about 30% less oxidant is
585 required, to fill the porosity of the soil, compared to a direct injection of oxidant liquids.
586 Even though the oxidant volumes were lower, the same HC degradation rates and the
587 isotropic distribution of reagents into the soil were achieved, using the foam-based method.
588 Since foam persists for several weeks into the soil [26,31], there is no need to inject foam
589 anymore.

590 Considering the foam injection process, a cheap foam generator was used. An accurate
591 monitoring of the injection pressures, flow rates and injected volumes would be required
592 when using the foam-based method. Yet, this kind of devices is commonly used during
593 remediation operations using routed SP. Thus, the cost balance is in favor of this innovative
594 foam-based method. Furthermore, another advantage is that the foam prevents harmful

595 vapors from being released, which usually occurs when the exothermic Fenton reaction is
596 used. Moreover, the use of the foam based-method leads to a more complete degradation
597 of the HCs [28].

598 4. Conclusions

599 The new foam-based technology is very effective to remediate HC contaminated
600 unsaturated soils, using *in situ* Fenton oxidation and biodegradation. It offers a better
601 controlled delivery of reagents solutions than their direct injection. Moreover, it fights
602 gravity effects, leading to a longer residence time of amendment in the vadose zone. Thanks
603 to a piston-like effect, solutions flow through the foam lamella network, avoiding nasty
604 interactions between the surfactant required to make foams and the very reactive oxidant
605 or surfactant-sensitive microorganisms. HC removal rates as high as 96% were obtained
606 using the acidic Fenton reagent. Yet, the coupling of Fenton with biological treatments,
607 without acidification, is effective and degradation rates as high as 75% were reached. Even if
608 the concentration of microorganisms decreased immediately after a non acidified Fenton
609 treatment, it was recovered within 40 d. Fieldworks were slightly delayed, because of the
610 foam injection and the high hydraulic resistance of the injection tool. Yet, the latter could be
611 improved. Moreover, it is important to consider a transient regime before getting the
612 homogeneous propagation of viscous foams. Regarding this, differential ERT is attractive to
613 track foam and amendment propagation at field-scale, but also their behaviour. This
614 monitoring suggests that the developed technology is quite robust towards risks of
615 uncontrolled delivery that may arise at high injection rates of reagents. This technology is
616 not more expensive than classical treatments. Moreover, it reduces treatment uncertainties
617 and the release of harmful vapors generated during the Fenton treatment. Yet, considering

618 the mobilization of some HC outside the treated zone, a remanent oxidant, like persulfate,
619 should be introduced both in the injected surfactant solution and in groundwater.

620 5. Acknowledgements

621 This research was carried out as a part of the MOUSTIC project funded by the French
622 National Research Agency (ANR-15-CE04-0011). Laura Fatin-Rouge is acknowledged for her
623 help to improve the English of the manuscript.

624 6. References

- 625 [1] D.W. Tomlinson, M.O. Rivett, G.P. Wealthall, R.E.H. Sweeney, Understanding complex
626 LNAPL sites: Illustrated handbook of LNAPL transport and fate in the subsurface, J.
627 Environ. Manage. 204 (2017) 748–756. doi:10.1016/j.jenvman.2017.08.015.
- 628 [2] M.A. Lominchar, A. Santos, E. de Miguel, A. Romero, Remediation of aged diesel
629 contaminated soil by alkaline activated persulfate, Sci. Total Environ. 622–623 (2018)
630 41–48. doi:10.1016/j.scitotenv.2017.11.263.
- 631 [3] J. Pinedo, R. Ibáñez, J.P.A. Lijzen, Á. Irabien, Assessment of soil pollution based on
632 total petroleum hydrocarbons and individual oil substances, J. Environ. Manage. 130
633 (2013) 72–79. doi:10.1016/j.jenvman.2013.08.048.
- 634 [4] V. Antoni, Basol : un panorama des sites et sols pollués, ou potentiellement pollués,
635 nécessitant une action des pouvoirs publics, Paris, 2013.
- 636 [5] R.L. Siegrist, M. Crimi, T.J. Simpkin, In Situ Chemical Oxidation for Groundwater
637 Remediation, Springer-Verlag, New York, 2011. doi:10.1007/978-1-4419-7826-4.

- 638 [6] M. Cheng, G. Zeng, D. Huang, C. Lai, P. Xu, C. Zhang, Y. Liu, Hydroxyl radicals based
639 advanced oxidation processes (AOPs) for remediation of soils contaminated with
640 organic compounds : A review, *Chem. Eng. J.* 284 (2016) 582–598.
641 doi:10.1016/j.cej.2015.09.001.
- 642 [7] J. Gryzenia, D. Cassidy, D. Hampton, Production and accumulation of surfactants
643 during the chemical oxidation of PAH in soil, *Chemosphere.* 77 (2009) 540–545.
644 doi:10.1016/j.chemosphere.2009.07.012.
- 645 [8] A. Goi, N. Kulik, M. Trapido, Combined chemical and biological treatment of oil
646 contaminated soil, *Chemosphere.* 63 (2006) 1754–1763.
647 doi:10.1016/j.chemosphere.2005.09.023.
- 648 [9] D. Huang, C. Hu, G. Zeng, M. Cheng, P. Xu, X. Gong, R. Wang, W. Xue, Combination of
649 Fenton processes and biotreatment for wastewater treatment and soil remediation,
650 *Sci. Total Environ.* 574 (2017) 1599–1610. doi:10.1016/j.scitotenv.2016.08.199.
- 651 [10] G.A. Silva-Castro, B. Rodelas, C. Perucha, J. Laguna, J. González-López, C. Calvo,
652 Bioremediation of diesel-polluted soil using biostimulation as post-treatment after
653 oxidation with Fenton-like reagents: Assays in a pilot plant, *Sci. Total Environ.* 445–
654 446 (2013) 347–355. doi:10.1016/j.scitotenv.2012.12.081.
- 655 [11] N.B. Sutton, T. Grotenhuis, H.H.M.M. Rijnaarts, Impact of organic carbon and
656 nutrients mobilized during chemical oxidation on subsequent bioremediation of a
657 diesel-contaminated soil, *Chemosphere.* 97 (2014) 64–70.
658 doi:10.1016/j.chemosphere.2013.11.005.

- 659 [12] R. Bajagain, Y. Park, S.W. Jeong, Feasibility of oxidation-biodegradation serial foam
660 spraying for total petroleum hydrocarbon removal without soil disturbance, *Sci. Total*
661 *Environ.* 626 (2018) 1236–1242. doi:10.1016/j.scitotenv.2018.01.212.
- 662 [13] S. Gan, E. V. Lau, H.K. Ng, Remediation of soils contaminated with polycyclic aromatic
663 hydrocarbons (PAHs), *J. Hazard. Mater.* 172 (2009) 532–549.
664 doi:10.1016/j.jhazmat.2009.07.118.
- 665 [14] B. Ranc, P. Faure, V. Croze, M.O. Simonnot, Selection of oxidant doses for in situ
666 chemical oxidation of soils contaminated by polycyclic aromatic hydrocarbons (PAHs):
667 A review, *J. Hazard. Mater.* 312 (2016) 280–297. doi:10.1016/j.jhazmat.2016.03.068.
- 668 [15] C. Trelu, E. Mousset, Y. Pechaud, D. Huguenot, E.D. Van Hullebusch, G. Esposito, M.A.
669 Oturan, Removal of hydrophobic organic pollutants from soil washing / flushing
670 solutions : A critical review, *J. Hazard. Mater.* 306 (2016) 149–174.
671 doi:10.1016/j.jhazmat.2015.12.008.
- 672 [16] F.H. Chapelle, P.M. Bradley, C.C. Casey, Behavior of a Chlorinated Ethene Plume
673 following Source-Area Treatment with Fenton’s Reagent, *Groundw. Monit. Remediat.*
674 (2005) 131–141. doi:https://doi.org/10.1111/j.1745-6592.2005.0020.x.
- 675 [17] N. Kulik, A. Goi, M. Trapido, T. Tuhkanen, Degradation of polycyclic aromatic
676 hydrocarbons by combined chemical pre-oxidation and bioremediation in creosote
677 contaminated soil, *J. Environ. Manage.* 78 (2006) 382–391.
678 doi:10.1016/j.jenvman.2005.05.005.
- 679 [18] C.M. Miller, R.L. Valentine, M.E. Roehl, P.J.J. Alvarez, Chemical and microbiological

- 680 assessment of pendimethalin-contaminated soil after treatment with Fenton's
681 reagent, *Water Res.* 30 (1996) 2579–2586. doi:[https://doi.org/10.1016/S0043-](https://doi.org/10.1016/S0043-1354(96)00151-0)
682 1354(96)00151-0.
- 683 [19] X. Xu, A. Saeedi, Evaluation and Optimization Study on a Hybrid EOR Technique
684 Named as Chemical-Alternating-Foam Floods, *Oil Gas Sci. Technol.* 72 (2017) 1–14.
685 doi:[10.2516/ogst/2016022](https://doi.org/10.2516/ogst/2016022).
- 686 [20] L.D. Hansen, C. Nestler, D. Ringelberg, R. Bajpai, Extended bioremediation of PAH/PCP
687 contaminated soils from the POPILE wood treatment facility, *Chemosphere.* 54 (2004)
688 1481–1493. doi:<https://doi.org/10.1016/j.chemosphere.2003.09.046>.
- 689 [21] Venny, S. Gan, H.K. Ng, Modified Fenton oxidation of polycyclic aromatic hydrocarbon
690 (PAH)-contaminated soils and the potential of bioremediation as post-treatment, *Sci.*
691 *Total Environ.* 419 (2012) 240–249. doi:[10.1016/j.scitotenv.2011.12.053](https://doi.org/10.1016/j.scitotenv.2011.12.053).
- 692 [22] S. Kuppusamy, P. Thavamani, K. Venkateswarlu, Remediation approaches for
693 polycyclic aromatic hydrocarbons (PAHs) contaminated soils : Technological
694 constraints , emerging trends and future directions, *Chemosphere.* 168 (2017) 944–
695 968. doi:[10.1016/j.chemosphere.2016.10.115](https://doi.org/10.1016/j.chemosphere.2016.10.115).
- 696 [23] N.B. Sutton, J.T.C. Grotenhuis, A.A.M. Langenhoff, H.H.M. Rijnaarts, Efforts to improve
697 coupled in situ chemical oxidation with bioremediation: A review of optimization
698 strategies, *J. Soils Sediments.* 11 (2011) 129–140. doi:[10.1007/s11368-010-0272-9](https://doi.org/10.1007/s11368-010-0272-9).
- 699 [24] S. Fuentes, V. Méndez, P. Aguila, M. Seeger, Bioremediation of petroleum
700 hydrocarbons : catabolic genes , microbial communities , and applications, *Appl*

- 701 Microbiol Biotechnol. 98 (2014) 4781–4794. doi:10.1007/s00253-014-5684-9.
- 702 [25] I. Bouzid, J. Maire, N. Fatin-Rouge, Comparative assessment of a foam-based oxidative
703 treatment of hydrocarbon-contaminated unsaturated and anisotropic soils,
704 Chemosphere. 233 (2019) 667–676. doi:10.1016/j.chemosphere.2019.05.295.
- 705 [26] I. Bouzid, J. Maire, S.I. Ahmed, N. Fatin-Rouge, Enhanced remedial reagents delivery in
706 unsaturated anisotropic soils using surfactant foam, Chemosphere. 210 (2018).
707 doi:10.1016/j.chemosphere.2018.07.081.
- 708 [27] L. Zhong, J. Szecsody, M. Oostrom, M. Truex, X. Shen, X. Li, Enhanced remedial
709 amendment delivery to subsurface using shear thinning fluid and aqueous foam, J.
710 Hazard. Mater. 191 (2011) 249–257. doi:10.1016/j.jhazmat.2011.04.074.
- 711 [28] I. Bouzid, J. Maire, N. Fatin-rouge, Comparative assessment of a foam-based method
712 for ISCO of coal tar contaminated unsaturated soils, J. Environ. Chem. Eng. 7 (2019)
713 103346. doi:10.1016/j.jece.2019.103346.
- 714 [29] J. Maire, A. Joubert, D. Kaifas, T. Invernizzi, J. Marduel, S. Colombano, D. Cazaux, C.
715 Marion, P. Klein, A. Dumestre, N. Fatin-rouge, Assessment of flushing methods for the
716 removal of heavy chlorinated compounds DNAPL in an alluvial aquifer, Sci. Total
717 Environ. 612 (2018) 1149–1158. doi:10.1016/j.scitotenv.2017.08.309.
- 718 [30] J. Maire, N. Fatin-Rouge, Surfactant foam flushing for in situ removal of DNAPLs in
719 shallow soils, J. Hazard. Mater. 321 (2017) 247–255.
720 doi:10.1016/j.jhazmat.2016.09.017.
- 721 [31] C. Portois, E. Essouayed, M.D. Annable, N. Guiserix, A. Joubert, O. Atteia, Field

722 demonstration of foam injection to confine a chlorinated solvent source zone, J.
723 Contam. Hydrol. 214 (2018) 16–23. doi:10.1016/j.jconhyd.2018.04.003.

724 [32] M. Longpré-girard, R. Martel, T. Robert, R. Lefebvre, J. Lauzon, 2D sandbox
725 experiments of surfactant foams for mobility control and enhanced LNAPL recovery in
726 layered soils, J. Contam. Hydrol. 193 (2016) 63–73.
727 doi:10.1016/j.jconhyd.2016.09.001.

728 [33] X. Shen, L. Zhao, Y. Ding, B. Liu, H. Zeng, L. Zhong, X. Li, Foam, a promising vehicle to
729 deliver nanoparticles for vadose zone remediation, J. Hazard. Mater. 186 (2011)
730 1773–1780. doi:10.1016/j.jhazmat.2010.12.071.

731 [34] K. Ma, R. Liontas, C.A. Conn, G.J. Hirasaki, S.L. Biswal, Visualization of improved sweep
732 with foam in heterogeneous media using microfluidics, Soft Matter. 8 (2012) 10669–
733 10675. doi:10.1039/c2sm25833a.

734 [35] G.J. Hirasaki, C.A. Miller, R. Szafranski, J. Lawson, N. Akiya, Surfactant/Foam Process
735 for Aquifer Remediation, in: Int. Symp. Oilf. Chem., Society of Petroleum Engineers,
736 Houston, Texas, 1997. doi:10.2118/37257-MS.

737 [36] J. Maire, A. Coyer, N. Fatin-rouge, Surfactant foam technology for in situ removal of
738 heavy chlorinated, J. Hazard. Mater. 299 (2015) 630–638.
739 doi:10.1016/j.jhazmat.2015.07.071.

740 [37] G.J. Hirasaki, C.A. Miller, R. Szafranski, J.B. Lawson, N. Akiya, Surfactant/foam process
741 for aquifer remediation, Proc. - SPE Int. Symp. Oilf. Chem. (1997) 471–480.
742 doi:10.2523/37257-ms.

- 743 [38] I. Bouzid, J. Maire, E. Brunol, S. Caradec, N. Fatin-Rouge, Compatibility of surfactants
744 with activated-persulfate for the selective oxidation of PAH in groundwater
745 remediation, *J. Environ. Chem. Eng.* 5 (2017) 6098–6106.
746 doi:10.1016/j.jece.2017.11.038.
- 747 [39] I. Watson, A. Burnett, *Hydrology: an Environmental Approach*, 1st Editio, CRC Press,
748 1995. doi:https://doi.org/10.1201/9780203751442.
- 749 [40] M. Fireman, Permeability Measurements On Disturbed Soil Samples, *Soil Sci.* 58
750 (1944) 337–354.
- 751 [41] M. Carter, E. Gregorich, *Soil sampling and methods of analysis*, 2nd editio, 2007.
752 doi:https://doi.org/10.1201/9781420005271.
- 753 [42] ISO 10390, *Soil quality — Determination of pH*, (2005).
- 754 [43] A. Dreimanis, Quantitative gasometric determination of calcite and dolomite by using
755 Chittick apparatus, *J. Sediment. Res.* 32 (1962) 520–529.
756 doi:https://doi.org/10.1306/74D70D08-2B21-11D7-8648000102C1865D.
- 757 [44] J. Bachmann, a Ellies, K.. Hartge, Development and application of a new sessile drop
758 contact angle method to assess soil water repellency, *J. Hydrol.* 231–232 (2000) 66–
759 75. doi:10.1016/S0022-1694(00)00184-0.
- 760 [45] K. Schöffski, D. Strohm, Karl Fischer Moisture Determination, *Encycl. Anal. Chem.*
761 (2006) 1–13. doi:10.1002/9780470027318.a8102.
- 762 [46] Standards Association of Australia, *Methods of testing soil for engineering purposes*
763 Part B - Soil moisture content tests - Determination of the moisture content of a soil -

- 764 Oven drying method (standard method), 1977.
- 765 [47] D.L. Sparks, A.L. Page, P.A. Helmke, R.H. Loeppert, *Methods of Soil Analysis, Part 3:*
766 *Chemical Methods*, John Wiley & Sons, 2020.
- 767 [48] S. Jorfi, A. Rezaee, N. Jaafarzadeh, Pyrene removal from contaminated soils by
768 modified Fenton oxidation using iron nano particles, *J. Environ. Heal. Sci. Eng.* 11
769 (2013) 2–9. doi:10.1186/2052-336X-11-17.
- 770 [49] H. Sun, Y. Qi-she, Influence of pyrene combination state in soils on its treatment
771 efficiency by Fenton oxidation, *J. Environ. Manage.* 88 (2008) 556–563.
772 doi:10.1016/j.jenvman.2007.03.031.
- 773 [50] M. Usman, P. Faure, C. Ruby, K. Hanna, Remediation of PAH-contaminated soils by
774 magnetite catalyzed Fenton-like oxidation, *Appl. Catal. B Environ.* 117–118 (2012) 10–
775 17. doi:10.1016/j.apcatb.2012.01.007.
- 776 [51] C. Valderrama, R. Alessandri, T. Aunola, J.L. Cortina, X. Gamisans, T. Tuhkanen,
777 Oxidation by Fenton’s reagent combined with biological treatment applied to a
778 creosote-contaminated soil, *J. Hazard. Mater.* 166 (2009) 594–602.
779 doi:10.1016/j.jhazmat.2008.11.108.
- 780 [52] H. Ouriache, J. Arrar, A. Namane, F. Bentahar, Treatment of petroleum hydrocarbons
781 contaminated soil by Fenton like oxidation, *Chemosphere.* 232 (2019) 377–386.
782 doi:10.1016/j.chemosphere.2019.05.060.
- 783 [53] B. Ranc, P. Faure, V. Croze, C. Lorgeoux, M. Simonnot, Comparison of the
784 effectiveness of soil heating prior or during in situ chemical oxidation (ISCO) of aged

- 785 PAH-contaminated soils, (2017) 11265–11278. doi:10.1007/s11356-017-8731-0.
- 786 [54] S.R. Kanel, B. Neppolian, H. Choi, J.-W. Yang, Heterogeneous Catalytic Oxidation of
787 Phenanthrene by Hydrogen Peroxide in Soil Slurry: Kinetics, Mechanism, and
788 Implication, *Soil Sediment Contam.* 12 (2003) 101–117. doi:10.1080/713610963.
- 789 [55] D.O. Pino-Herrera, Y. Fayolle, S. Pageot, D. Huguenot, G. Esposito, E.D. van
790 Hullebusch, Y. Pechaud, Gas-liquid oxygen transfer in aerated and agitated slurry
791 systems with high solid volume fractions, *Chem. Eng. J.* 350 (2018) 1073–1083.
792 doi:10.1016/j.cej.2018.05.193.
- 793 [56] C.A. Schneider, W.S. Rasband, K.W. Eliceiri, NIH Image to ImageJ : 25 years of image
794 analysis, *Nat. Methods.* 9 (2012) 671–675. doi:10.1038/nmeth.2089.
- 795 [57] US EPA, Hydraulic fracturing technology, EPA 540-R-93-505. (1993) 140.
- 796 [58] Y. Wu, S. Hubbard, D. Wellman, Geophysical Monitoring of Foam Used to Deliver
797 Remediation Treatments within the Vadose Zone, *Vadose Zo. J.* 11 (2012) 0.
798 doi:10.2136/vzj2011.0160.
- 799 [59] V. Bichet, E. Grisey, Spatial characterization of leachate plume using electrical
800 resistivity tomography in a land fill composed of old and new cells (Belfort , France),
801 211 (2016) 61–73. doi:10.1016/j.enggeo.2016.06.026.
- 802 [60] J.T. Woods, M.G. Mellon, Thiocyanate Method for Iron A Spectrophotometric Study,
803 *Ind. Eng. Chem. - Anal. Ed.* 13 (1941) 551–554. doi:10.1021/i560096a013.
- 804 [61] P. Vähöja, K. Roppola, I. Välimäki, T. Kuokkanen, Studies of biodegradability of
805 certain oils in forest soil as determined by the respirometric BOD OxiTop method, *Int.*

806 J. Environ. Anal. Chem. 85 (2005) 1065–1073. doi:10.1080/03067310500174195.

807 [62] I.L. Pepper, C.P. Gerba, T.J. Gentry, R.M. Maier, *Environmental Microbiology*,
808 Academic Press, 2011.

809 [63] R.K. Rothmel, R.W. Peters, E. St. Martin, M.F. Deflaun, *Surfactant*
810 *foam/bioaugmentation technology for in situ treatment of TCE- DNAPLs*, *Environ. Sci.*
811 *Technol.* 32 (1998) 1667–1675. doi:10.1021/es970980w.

812 [64] S. Hashemian, M. Tabatabaee, M. Gafari, *Fenton oxidation of methyl violet in aqueous*
813 *solution*, *J. Chem.* (2013). doi:10.1155/2013/509097.

814 [65] S. Hashemian, *Fenton-like oxidation of malachite green solutions: Kinetic and*
815 *thermodynamic study*, *J. Chem.* 2013 (2013). doi:10.1155/2013/809318.

816 [66] A. Bharadwaj, A.K. Saroha, *Decolorization of the textile wastewater containing*
817 *reactive blue 19 dye by Fenton and Photo-Fenton oxidation*, *J. Hazardous, Toxic,*
818 *Radioact. Waste.* 19 (2015) 1–7. doi:10.1061/(ASCE)HZ.2153-5515.0000267.

819 [67] Y.S. Jung, W.T. Lim, J.Y. Park, Y.H. Kim, *Effect of pH on Fenton and Fenton - like*
820 *oxidation*, *Environ. Technol.* 30 (2009) 183–190. doi:10.1080/09593330802468848.

821 [68] C. Chang, Y. Hsieh, K. Cheng, L. Hsieh, *Effect of pH on Fenton process using estimation*
822 *of hydroxyl radical with salicylic acid as trapping reagent*, *Water Sci. Technol.* 54
823 (2008) 873–879. doi:10.2166/wst.2008.429.

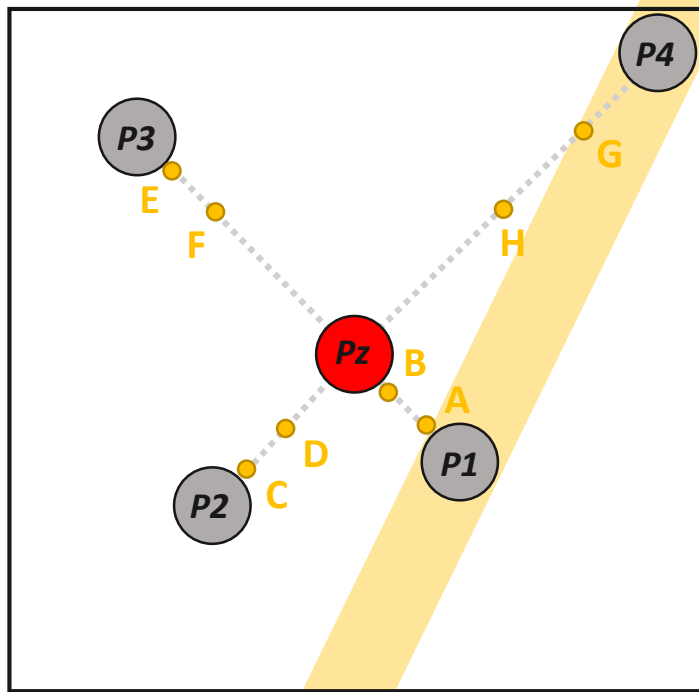
824 [69] Y.S. Zhao, Y. Su, J.R. Lian, H.F. Wang, L.L. Li, C.Y. Qin, *Insights on Flow Behavior of*
825 *Foam in Unsaturated Porous Media during Soil Flushing*, *Water Environ. Res.* 88
826 (2016) 2132–2141. doi:10.2175/106143016X14733681695483.




- 827 [70] K. Nam, W. Rodriguez, J.J. Kukor, Enhanced degradation of polycyclic aromatic
828 hydrocarbons by biodegradation combined with a modified Fenton reaction,
829 Chemosphere. 45 (2001) 11–20. doi:10.1016/S0045-6535(01)00051-0.
- 830 [71] K. Osei-bonsu, N. Shokri, P. Grassia, Foam stability in the presence and absence of
831 hydrocarbons: From bubble- to bulk-scale, Colloids Surfaces A Physicochem. Eng. Asp.
832 481 (2015) 514–526. doi:10.1016/j.colsurfa.2015.06.023.
- 833 [72] C.S. Boeije, C. Portois, M. Schmutz, O. Atteia, Tracking a Foam Front in a 3D,
834 Heterogeneous Porous Medium, Transp. Porous Media. 131 (2018) 1–20.
835 doi:10.1007/s11242-018-1185-0.

836

837

Top view



-  Injection well
-  Observation well
- A to H* Soil sampling
-  ERT monitoring



Treatment steps

